PNAS

Supporting Information for:
Keratinocyte-TRPV1 sensory neuron interactions in a genetically controllable mouse model of chronic neuropathic itch

Andrew J. Crowther[1,6], Sakeen W. Kashem[2,3,6], Madison E. Jewell[1], Henry Le Chang, Élora Midavaine[1], Mariela Rosa Casillas[1],Veronika Danchine[2], Sian Rodriguez[1], Artur Kania[4], Ritchie Chen[5], Joao M. Braz[1], Allan I. Basbaum[1,*]

Affiliations:
[1]Department of Anatomy, University of California San Francisco, San Francisco, CA 94158, USA
[2]Department of Dermatology, University of California San Francisco, San Francisco, CA 94158, USA
[3]Division of Dermatology, San Francisco Veteran's Administration Healthcare System, San Francisco, CA 94121, USA
[4]Institut de Recherches Cliniques de Montréal (IRCM), Montreal, Qc, H2W 1R7
[5]Department of Neurological Surgery, University of California San Francisco, San Francisco, CA 94158, USA
[6]These authors contributed equally

[*]**Correspondence:**
Allan I. Basbaum, PhD
Professor and Chair
Department of Anatomy
University of California – San Francisco
allan.basbaum@ucsf.edu

This PDF file includes:

Figures S1 to S10
Legend for Movie S1

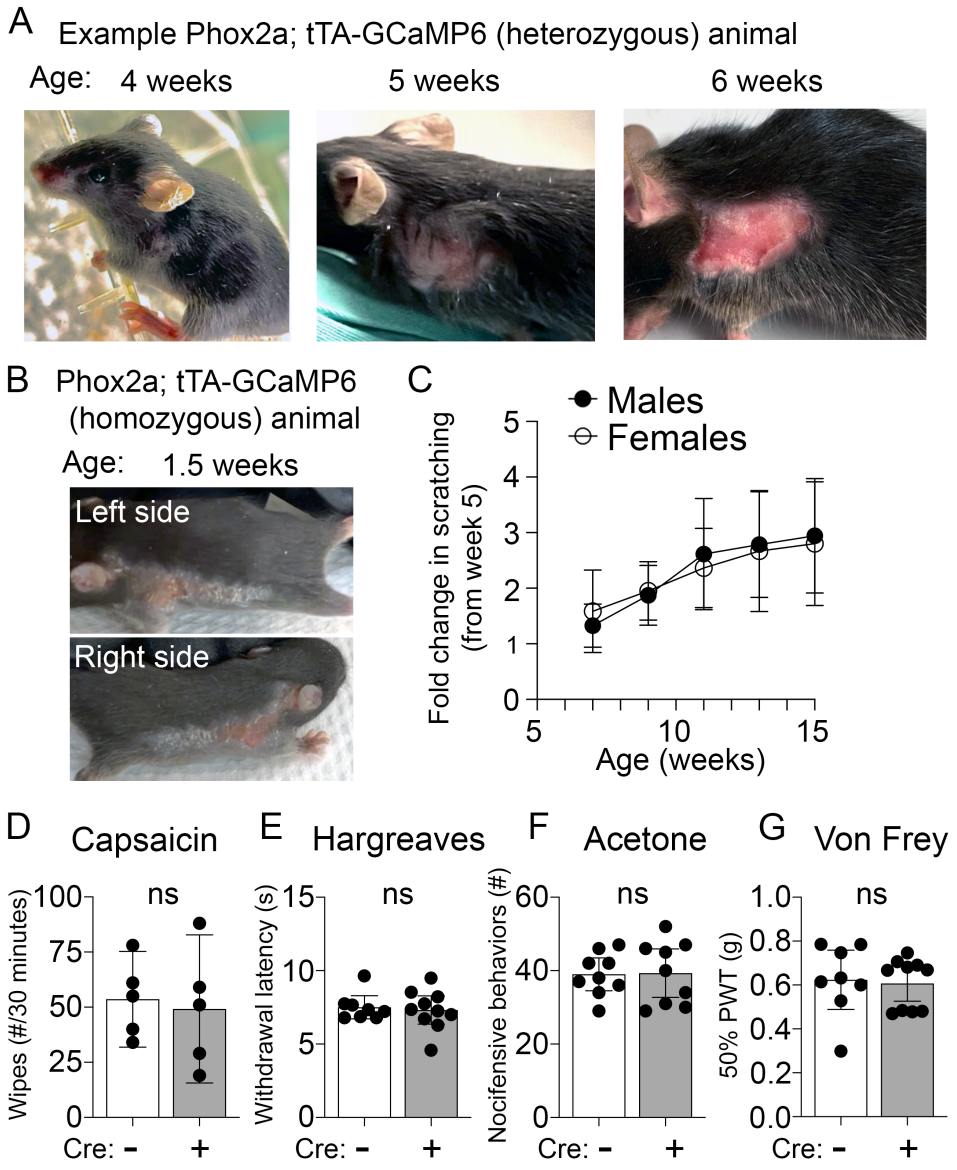

Figure S1. Additional characterization of the itch phenotype.
(A) A strong example of rapid lesion development in a Phox2a; tTA-GCaMP6 animal. This animal, like all animals in the study besides the mouse in (B), is heterozygous for the tTA-GCaMP6 allele. **(B)** Doubling the allele of tTA-GCaMP6 to homozygosity accelerates skin pathology of the shoulder area, now visible in an unweaned mouse pup. **(C)** Similar progression of scratching over time in male and female Phox2a; tTA-GCaMP6 mice. Data are normalized to initial scratching measurements at 5 weeks of age. Females (N=6), Males (N=7). **(D-G)** No significant differences observed between Cre+; tTA-GCaMP6 mice and Cre- littermate controls in: **(D)** capsaicin-injection-induced nocifensive behaviors (face wiping), **(E)** Hargreaves heat sensitivity, **(F)** acetone noxious cold sensitivity, or **(G)** Von Frey mechanical threshold. E-G were performed on the hind paws. Statistical analysis was performed using two-tailed unpaired t-tests. Error bars represent 95% Confidence Intervals. ns = non-significant.

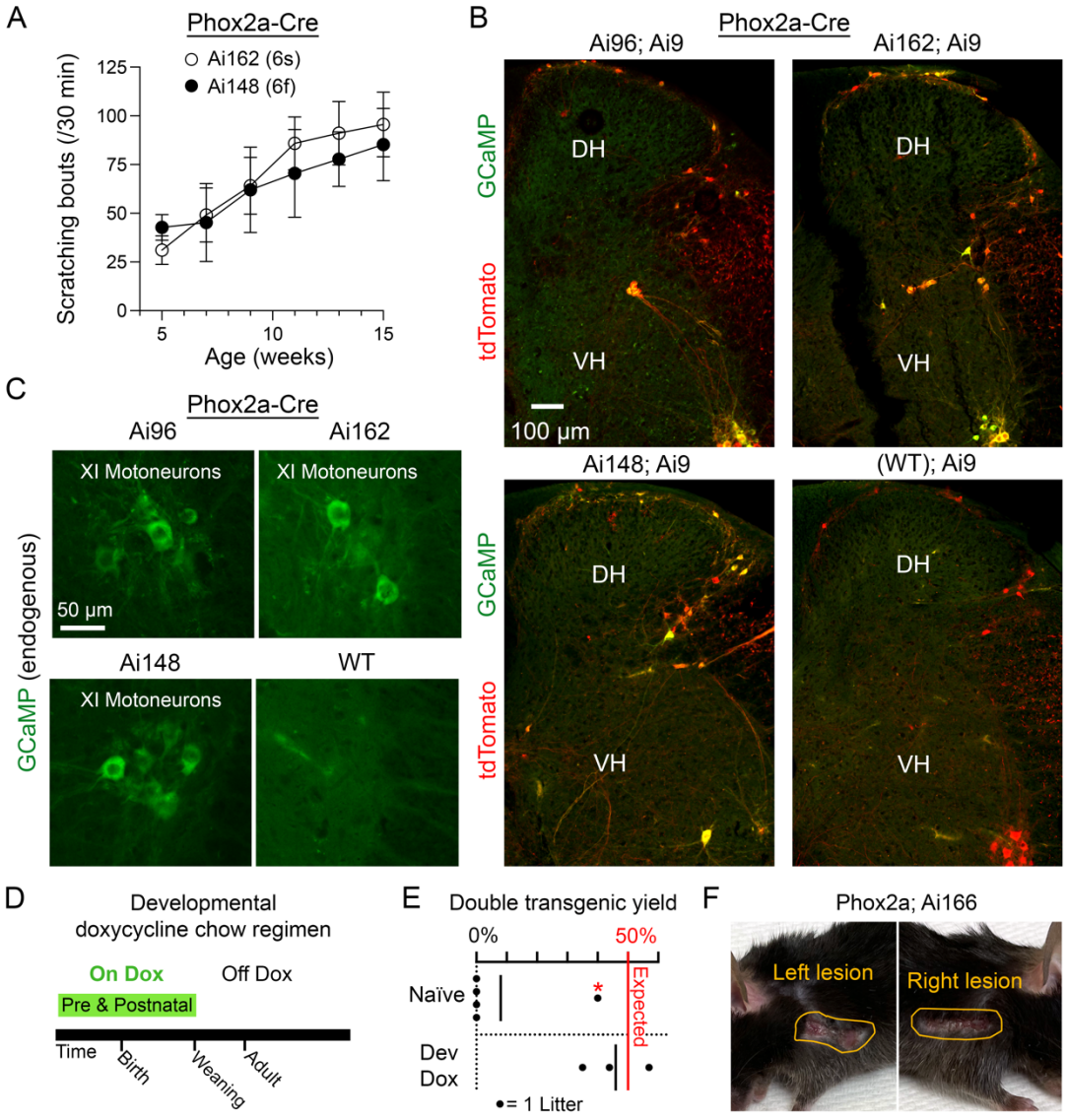

Figure S2. Cre-dependent reporter expression and tTA inhibition.
(A) Scratching progression compared between mice expressing fast (Ai162, N=9) and slow (Ai148, N=4) variants of GCaMP6. **(B)** Composite fluorescence images showing neuronal GCaMP (green) and tdTomato (red) expression in the cervical spinal cord across indicated GCaMP6 genotypes. tdTomato+ neurons in all genotypes confirm Cre recombination activity. **(C)** Cytoplasmic GCaMP6 expression in cervical XI motoneuron populations, missing in Phox2a-Cre mice without Ai162. **(D)** Scheme of doxycycline chow administration to inhibit tTA activity during development. **(E)** The mean yield of viable double transgenic mice per litter was only 13% without doxycycline compared to 46% with developmental doxycycline treatment (expected Mendelian yield is 50%, red line). One untreated litter (red asterisk) produced viable Phox2a-Cre; Ai166 mice that developed spontaneous scratching and skin lesions. **(F)** Representative images of these mice at 11 weeks of age show bilateral shoulder skin lesions (also see Figure 2E). Error bars indicate 95% Confidence Intervals. DH = Dorsal horn. VH = Ventral horn.

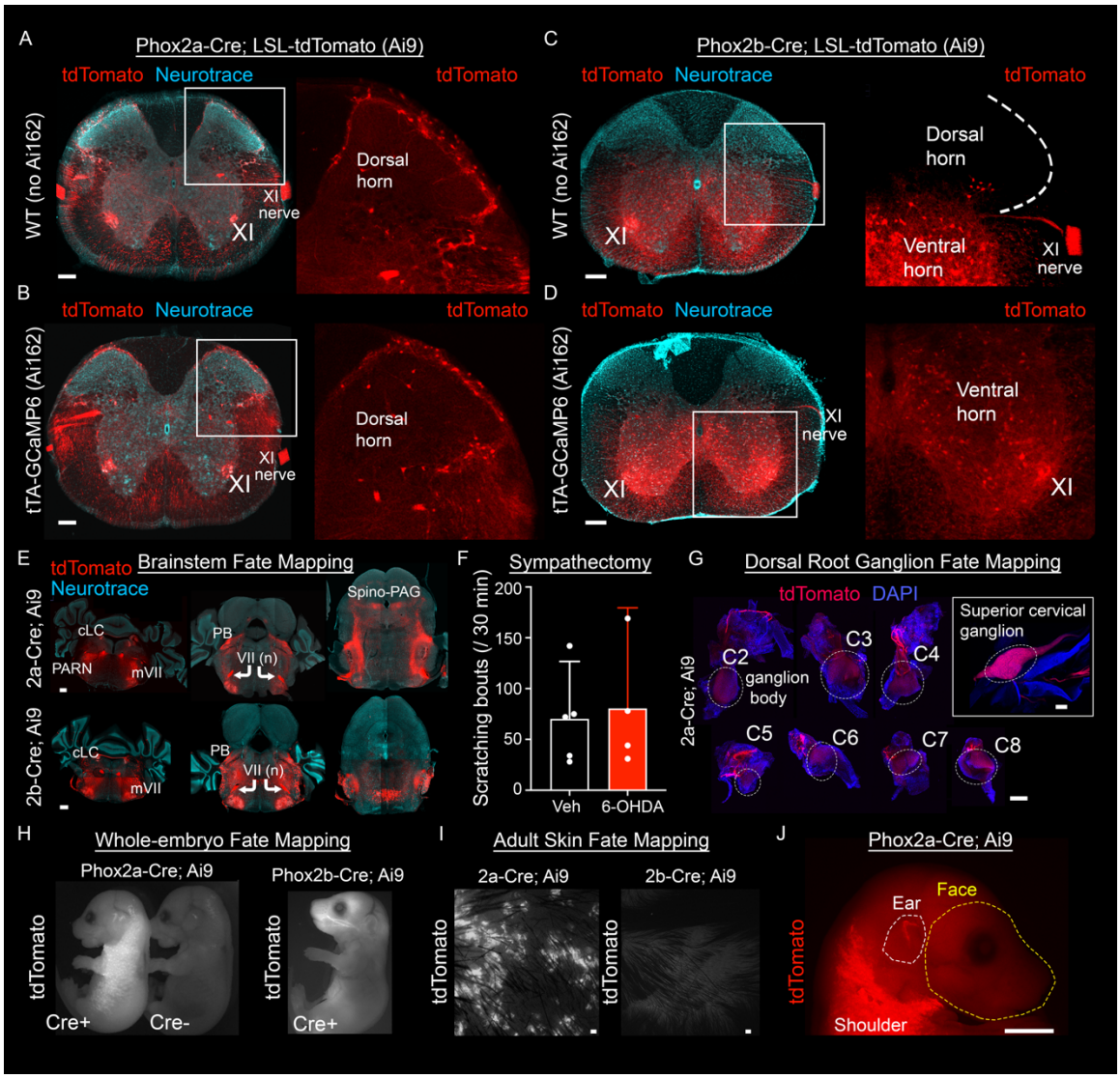

Figure S3. Additional Phox2a-Cre and Phox2b-Cre lineage fate mapping in the nervous system and skin.

(A) At the cervical spinal cord level, Phox2a-Cre fate-mapped tdTomato+ neurons in control mice are found in their typical laminae I and V, and XI motoneuron locations. **(B)** Phox2a-Cre; tTA-GCaMP6 neurons show similar localization and morphology to (A). **(C)** In Phox2b-Cre; Ai9 mice, the XI motoneuron pool and other neurons in the ventral horn are tdTomato+, but notably missing in the dorsal horn. **(D)** Phox2b-Cre; tTA-GCaMP6 neurons show similar localization and morphology to (C). **(E)** Comparative analysis of Phox2a- and Phox2b-Cre lines reveals overlapping neural recombination in the brainstem: mVII = facial motor nucleus, VII (n) = facial nerve, PARN = parvicellular reticular nucleus, cLC = caudal portion of the locus coeruleus, and PB = parabrachial nucleus. Spino-PAG indicates ascending terminals of dorsal horn projection neurons that are exclusively found in Phox2a-Cre mice. **(F)** Scratching analysis of Phox2a-Cre; Ai162 mice 1 month after 6-OHDA-induced sympathectomy (red bar) compared to littermate Phox2a-Cre; Ai162 mice that only received the vehicle (clear bar). Data points represent individual animals. Error bars are the 95% CI. **(G)** Cervical DRGs (outlined by dotted circle) lack tdTomato+ neurons in Phox2a-Cre mice, while the superior cervical ganglion

(inset) displays robust tdTomato labeling. Scale bars = 200 μm. **(H)** Skin tdTomato signal (white) is found in (~E18) Phox2a-Cre; Ai9 embryos (left) but not in Cre- embryos (middle) or Phox2b embryos (right). **(I)** The expression of tdTomato+ keratinocytes was confirmed in adult shoulder skin of Phox2a-Cre, but not Phox2b-Cre, Ai9 mice. **(J)** Magnification of the head region of a Phox2a-Cre; Ai9 embryo. tdTomato signal (red) is confluent at the shoulder and detectable at the tip of the ear; in contrast, the face shows minimal to no expression. Dotted lines in respective white or yellow colors outline the ear and face. Scale bars = 100 μm (A-E,I), 1000 μm (J).

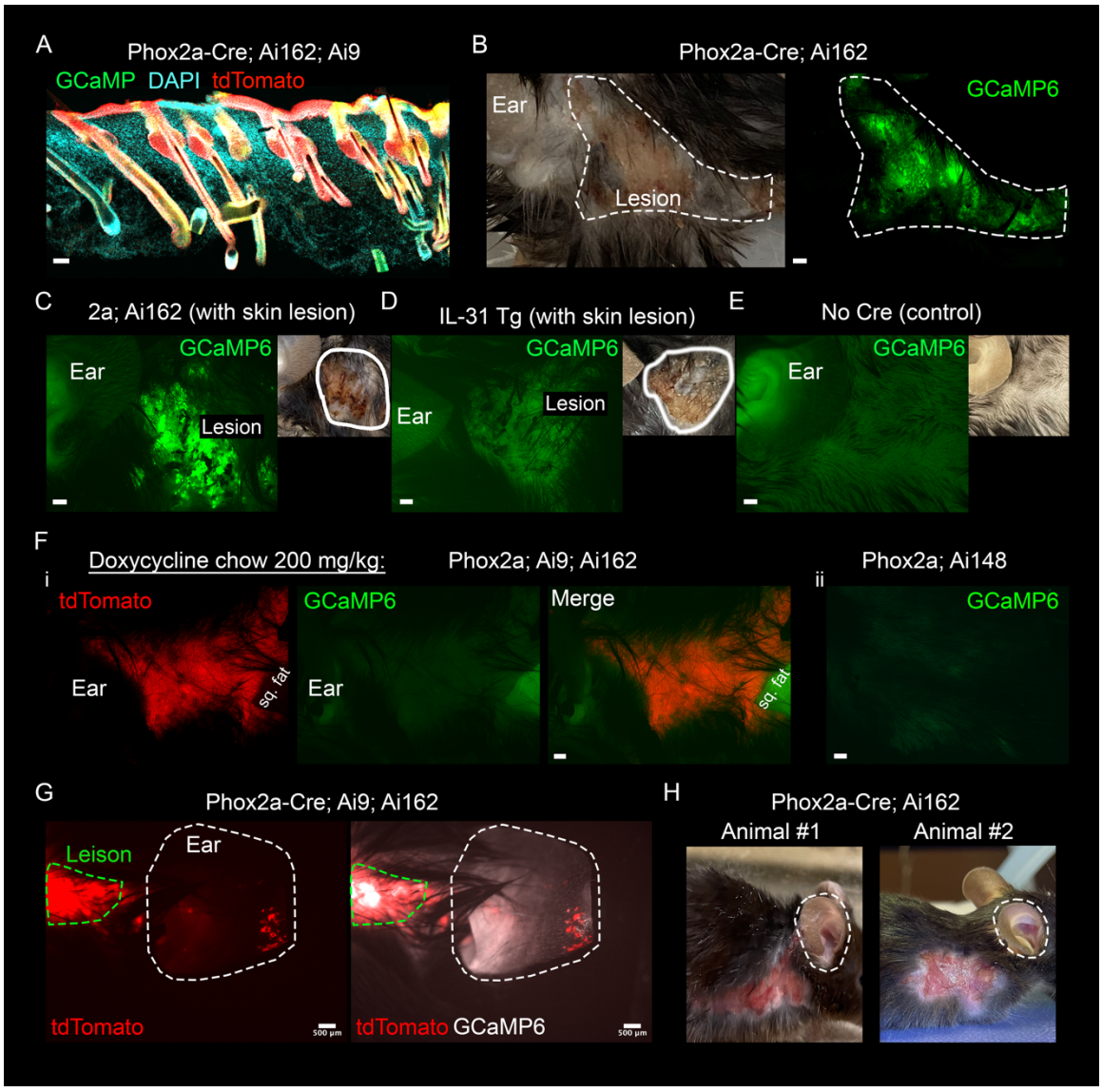

Figure S4. GCaMP6 and tdTomato expression in the skin of Phox2a-Cre mice. **(A)** Cross-section of shoulder skin from a 9-week-old adult Phox2a; Ai162; Ai9 mouse showing co-expression of GCaMP6 (green) and tdTomato (red) in Phox2a-keratinocytes throughout the epidermis and hair follicles. **(B)** GCaMP6 expression localized to skin lesion sites in a Phox2a-Cre; Ai162 mouse. A white dotted line marks the lesion boundary. **(C-E)** Wide-field fluorescence images (left) with corresponding true color photographs (right) of skin conditions in different mouse genotypes. (C-D) A white line in the true color image marks the lesion boundary. **(C)** Intralesional GCaMP6 fluorescence in a Phox2a-Cre; Ai162 mouse is compared to **(D)** idiopathic skin lesions from an IL-31 transgenic mouse (negative control) and **(E)** an Ai162 mouse without Cre (negative control). **(F)** Doxycycline effects: (i) In a doxycycline-treated Phox2a; Ai162; Ai9 mouse, tdTomato expression (red) persists while GCaMP6 is repressed. Phox2a-keratinocytes would co-express both reporters without doxycycline treatment. (ii) Similarly, an Ai148 mouse actively maintained on doxycycline chow shows no detectable GCaMP6 signal in the skin. **(G)** Whole-mount skin preparation of a Phox2a-Cre; Ai9; Ai162 mouse. tdTomato+ cells (red) are visible at the ear tip and more densely at the shoulder lesion,

with overlapping GCaMP6 signal (white). **(H)** The ears (white dotted line) appear normal in two Phox2a-Cre; Ai162 mice despite these animals having significant shoulder skin lesions. Scale bars = 100 μm (A), 1000 μm (B-H), 500 μm (G).

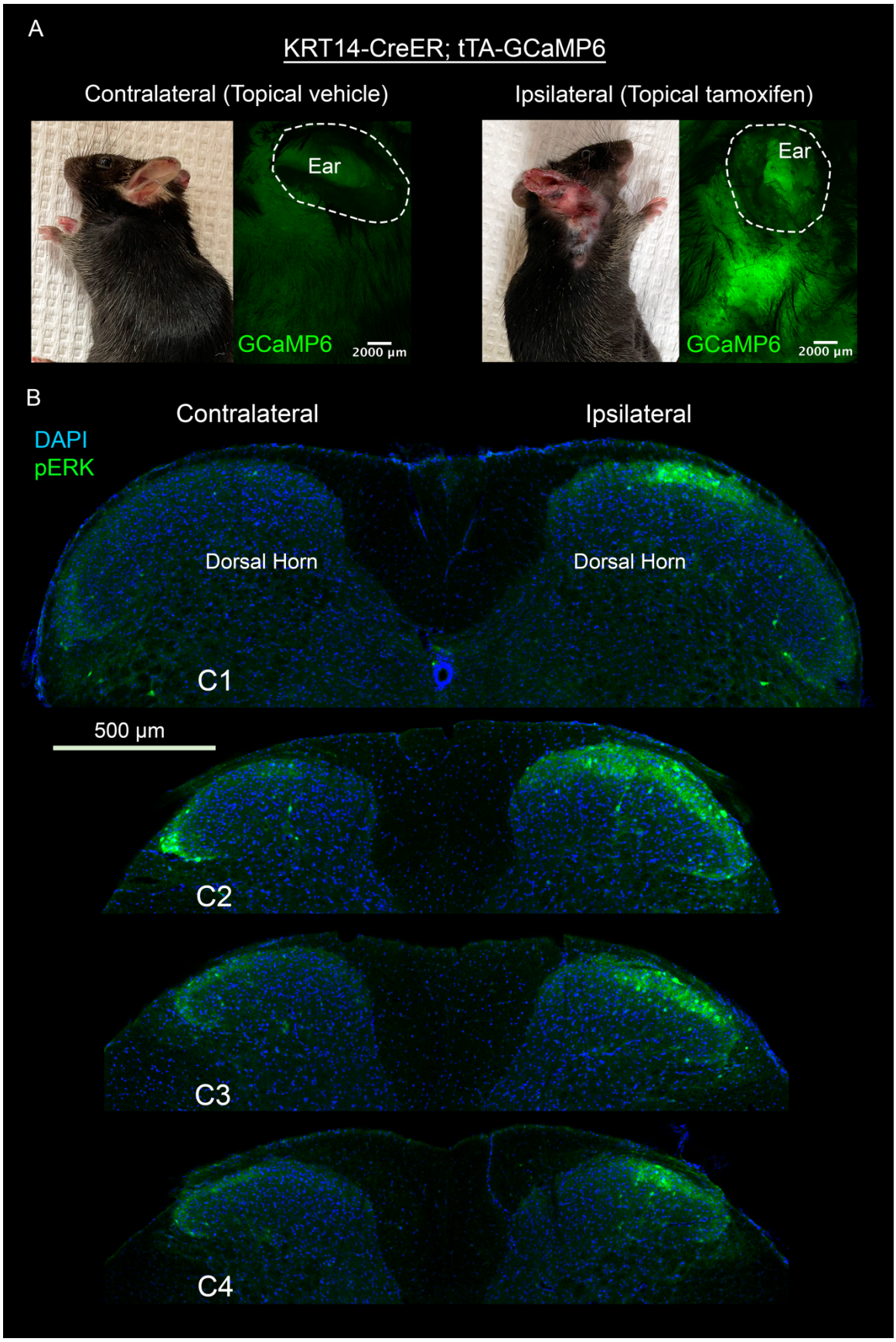
A
KRT14-CreER; tTA-GCaMP6
Contralateral (Topical vehicle)
Ipsilateral (Topical tamoxifen)
Ear
GCaMP6
2000 µm
Ear
GCaMP6
2000 µm
B
Contralateral
Ipsilateral
DAPI
pERK
Dorsal Horn
Dorsal Horn
C1
500 µm
C2
C3
C4

Figure S5. Unilateral tTA activation in KRT14-CreER mice produces ipsilateral skin lesions and dorsal horn activation.
(A) Left and right sides of a KRT-CreER; Ai162 mouse after unilateral 4-hydroxytamoxifen application. True color photos (left) show skin appearance, while fluorescence images (right) reveal GCaMP6 expression only on the treated side, including the shoulder and ear regions, correlating with skin lesions. **(B)** Phospho-ERK1/2 immunohistochemistry of cervical spinal cord sections from the same mouse. Images show the dorsal spinal cord at multiple cervical levels (C1-C4), with increased pERK immunoreactivity in the superficial laminae ipsilateral to tTA activation.

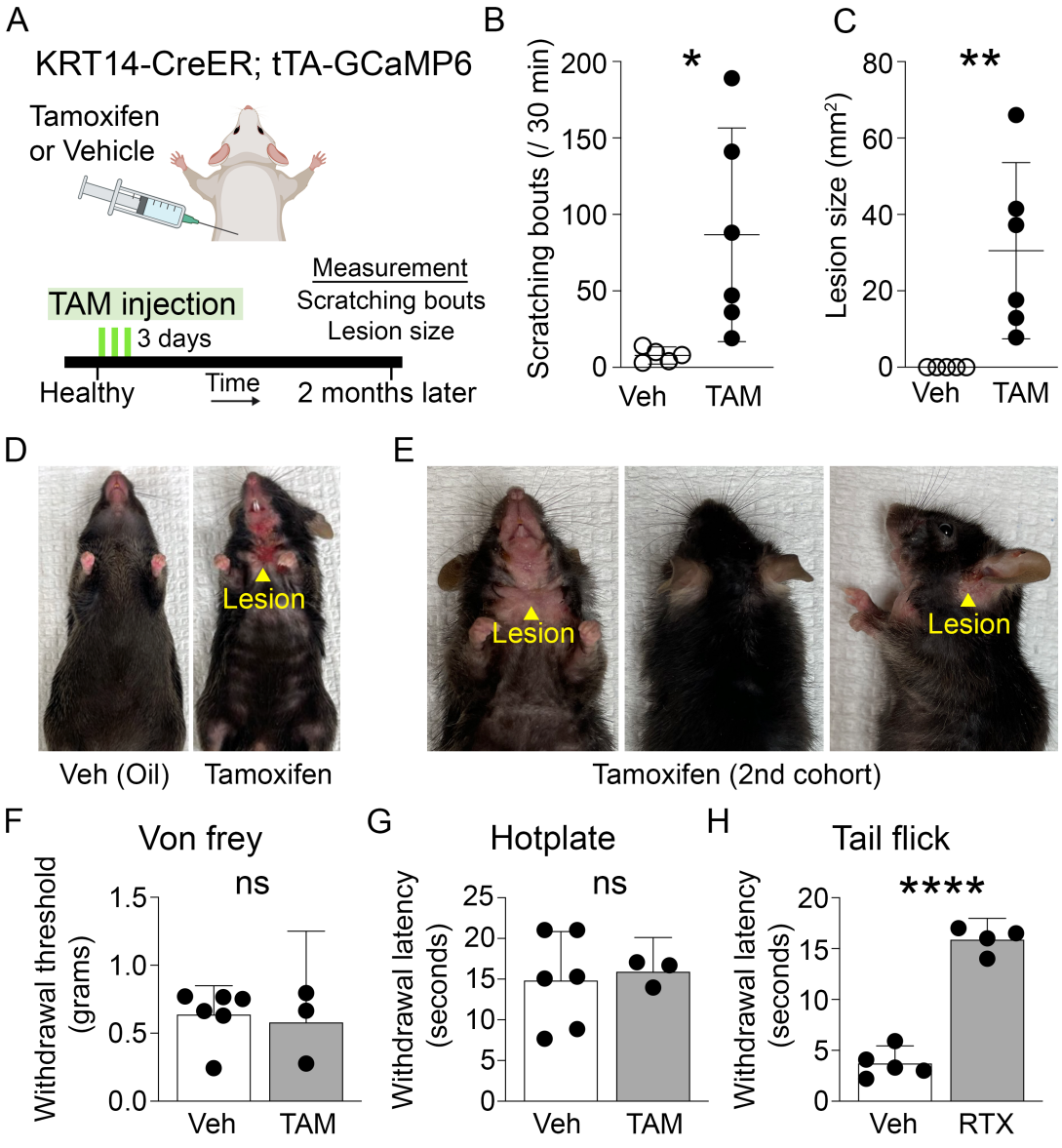

Figure S6. Systemic tTA activation in KRT14-CreER; tTA-GCaMP6 mice produces scratching and skin lesions.
(A-G) Effects of systemic tTA activation in Keratin14-expressing cells. **(A)** An experimental timeline schematic shows the ip. tamoxifen injection protocol and behavioral assessment schedule. (B-C) Quantification of **(B)** spontaneous scratching frequency and **(C)** skin lesion size in tamoxifen-treated versus vehicle (corn oil)-treated KRT14-CreER; Ai162 mice. **(D)** Representative photographs showing skin phenotypes at 3 months post-injection in vehicle-treated (left) versus tamoxifen-treated (right) mice. **(E)** Close-up images highlight the development of skin lesions at the ventral neck and ear in a second cohort of KRT14-CreER; Ai162 mice. **(F-G)** Sensory testing demonstrates that systemic tTA activation in keratinocytes does not alter general somatosensation. **(F)** Mechanical withdrawal thresholds measured by von Frey testing of the hind paw and **(G)** thermal withdrawal latencies measured by Hargreaves assay remained unchanged in tamoxifen-treated KRT14-CreER; Ai162 mice compared to

controls. **(H)** Validation of resiniferatoxin (RTX)-induced ablation of TRPV1-expressing afferents, as used in Figure 4I-K. Heat withdrawal latency was significantly increased in RTX-treated mice compared to vehicle-treated controls, confirming the successful ablation of TRPV1+ thermal nociceptors. Statistics were analyzed by two-tailed unpaired t-tests (B-C, F-H). Error bars indicate the 95% Confidence Interval. * $p < 0.05$, ** $p < 0.01$, **** $p < 0.0001$, ns = non-significant.

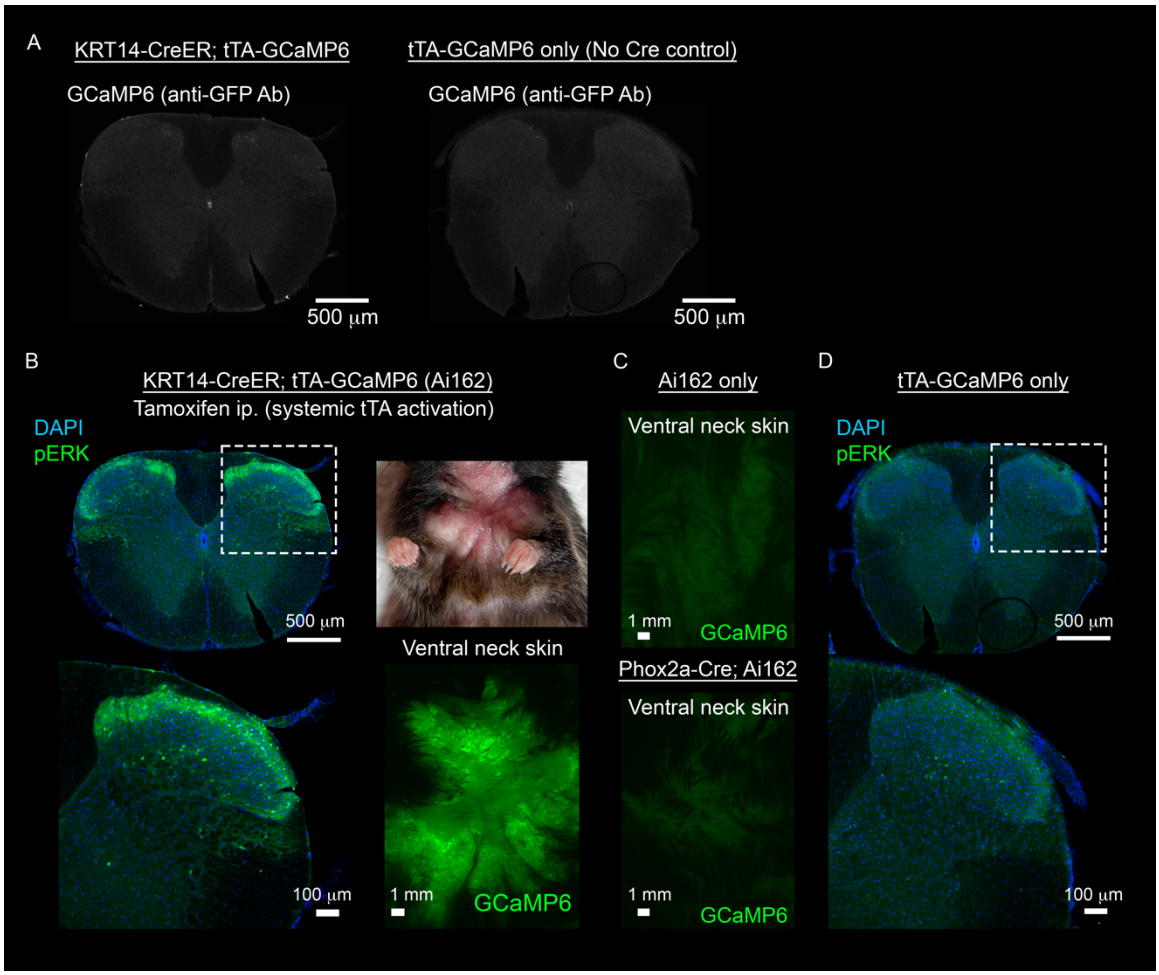

Figure S7. Skin GCaMP6 expression and dorsal horn activation in systemically activated KRT14CreER; tTA-GCaMP6 mice.
(A) Immunolabeling demonstrates the specificity of the KRT14-CreER line. No GCaMP6 expression is detected in cervical spinal cord neurons of tamoxifen-treated KRT14-CreER; Ai162 mice (left), matching the absence of labeling in Cre-negative control mice (right). These cervical sections correspond to the same mice and spinal levels shown in panels B and D, respectively. **(B)** Cervical spinal cord section from a tamoxifen-injected KRT14-CreER; Ai162 mouse showing robust pERK immunoreactivity in the superficial laminae of the dorsal horn bilaterally. This bilateral pattern of dorsal horn activation corresponds with the bilateral skin lesions at the ventral neck region displayed in the adjacent photograph. Whole-mount skin imaging (bottom right) confirms GCaMP6 expression in the ventral neck skin of this mouse, verifying tTA activation in keratinocytes. **(C)** Whole-mount fluorescence imaging of ventral neck skin from mice of different genotypes. Unlike the robust GCaMP6 signal observed at the ventral neck skin in KRT14-CreER, Ai162 mice (B), minimal fluorescence is detected in Cre-negative controls (top) or Phox2a-Cre, Ai162 mice (bottom) at this anatomical location. **(D)** A representative cervical spinal cord section from a Cre-negative littermate showing minimal pERK immunoreactivity in superficial dorsal horn laminae, in contrast to the robust signal seen in the KRT14-CreER; Ai162 mouse (B).

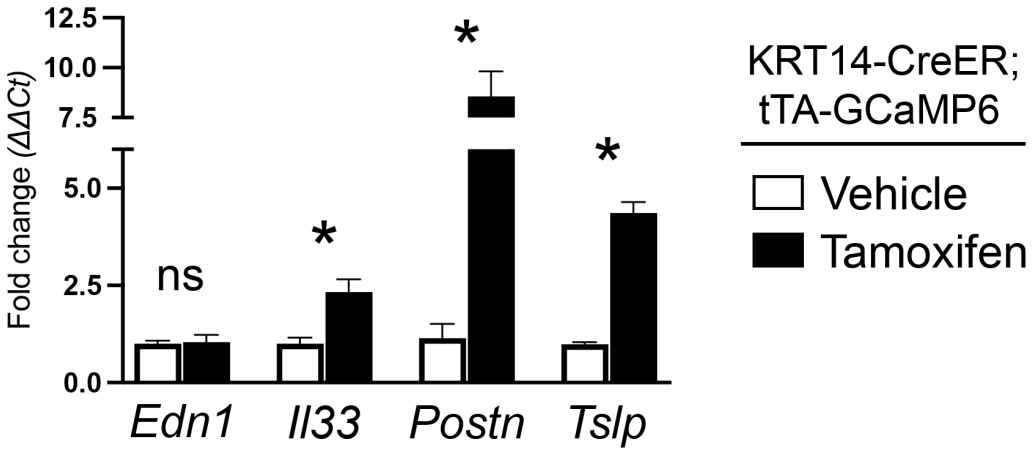

Figure S8. Upregulation of keratinocyte-associated pruritogenic factors in the ventral skin of KRT14-CreER mice with systemic tTA activation.
Targeted qPCR analysis of known pruritogenic mediators in lesional skin from tamoxifen-treated KRT14-CreER; Ai162 mice compared to control skin from vehicle (EtOH)-injected isogenotyped littermates. Relative expression levels were calculated using the 2−ΔΔCT method with β-actin as the internal control for each sample (N=4 per group). Statistical analysis was performed using the Mann-Whitney test; * $p < 0.05$.

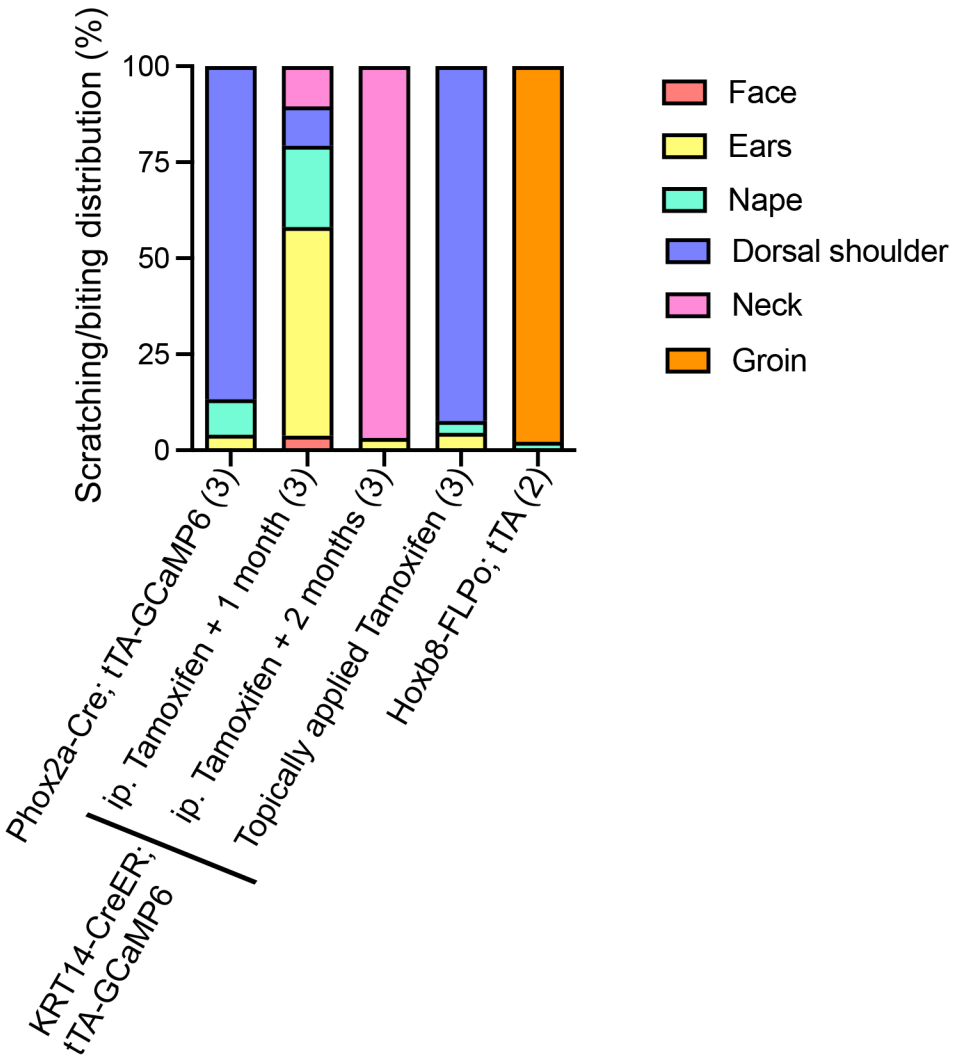

Figure S9. Scratching location is determined by the Cre/FLP driver line and evolves temporally in KRT14-CreER; tTA-GCaMP6 mice.
Quantification of behavior directed at different body regions, shown as a percentage of total behavior per mouse. The spatial pattern of scratching or biting/licking varies distinctly across different Cre/FLP driver lines used to activate tTA expression, demonstrating a strong correlation between keratinocyte tTA activation sites and targeted behaviors. Sample sizes are indicated in parentheses.

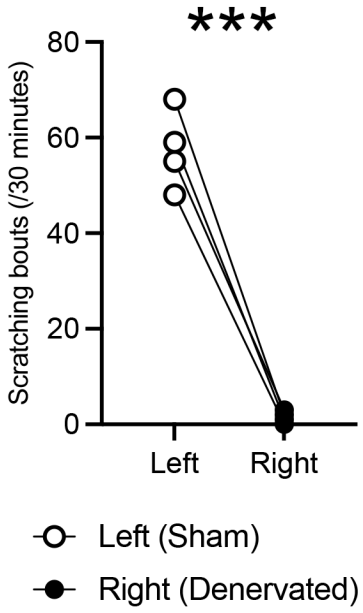

Figure S10. Peripheral sensory input maintains localized scratching in Phox2a; tTA-GCaMP6 mice.
Unilateral cutaneous denervation was performed on the right shoulder in Phox2a; tTA-GCaMP6 mice with established bilateral scratching and skin lesions. Scratching was measured at four days post-denervation. Connected points represent paired measurements from individual mice. Statistical significance was determined using a paired t-test (*** $p < 0.001$).

Movie S1 (separate file). Systemic, inducible activation of tTA triggers scratching in KRT14-CreER; tTA-GCaMP6 mice.
Example video showing three 8-week-old KRT14-CreER; tTA-GCaMP6s mice, recorded 1 month after intraperitoneal tamoxifen administration. The tamoxifen treatment activated tTA-GCaMP6 expression selectively in keratin14-expressing epithelial cells throughout the skin.